

## Evaporation of traffic-generated nanoparticles during advection from source

Harrison, Roy M.; Jones, Alan M.; Beddows, David C S; Dall'Osto, Manuel; Nikolova, Irina

DOI:

[10.1016/j.atmosenv.2015.10.077](https://doi.org/10.1016/j.atmosenv.2015.10.077)

License:

Creative Commons: Attribution (CC BY)

*Document Version*

Publisher's PDF, also known as Version of record

*Citation for published version (Harvard):*

Harrison, RM, Jones, AM, Beddows, DCS, Dall'Osto, M & Nikolova, I 2016, 'Evaporation of traffic-generated nanoparticles during advection from source', *Atmospheric Environment*, vol. 125, no. Part A, pp. 1-7.  
<https://doi.org/10.1016/j.atmosenv.2015.10.077>

[Link to publication on Research at Birmingham portal](#)

### General rights

Unless a licence is specified above, all rights (including copyright and moral rights) in this document are retained by the authors and/or the copyright holders. The express permission of the copyright holder must be obtained for any use of this material other than for purposes permitted by law.

- Users may freely distribute the URL that is used to identify this publication.
- Users may download and/or print one copy of the publication from the University of Birmingham research portal for the purpose of private study or non-commercial research.
- User may use extracts from the document in line with the concept of 'fair dealing' under the Copyright, Designs and Patents Act 1988 (?)
- Users may not further distribute the material nor use it for the purposes of commercial gain.

Where a licence is displayed above, please note the terms and conditions of the licence govern your use of this document.

When citing, please reference the published version.

### Take down policy

While the University of Birmingham exercises care and attention in making items available there are rare occasions when an item has been uploaded in error or has been deemed to be commercially or otherwise sensitive.

If you believe that this is the case for this document, please contact [UBIRA@lists.bham.ac.uk](mailto:UBIRA@lists.bham.ac.uk) providing details and we will remove access to the work immediately and investigate.



# Evaporation of traffic-generated nanoparticles during advection from source



Roy M. Harrison<sup>a,\*</sup>, Alan M. Jones<sup>a</sup>, David C.S. Beddows<sup>a</sup>, Manuel Dall'Osto<sup>b</sup>, Irina Nikolova<sup>a</sup>

<sup>a</sup> Division of Environmental Health and Risk Management, School of Geography, Earth and Environmental Sciences, University of Birmingham, Edgbaston, Birmingham B15 2TT, United Kingdom

<sup>b</sup> Institut de Ciències del Mar, CSIC, Pg Marítim de la Barceloneta 37–49, 08003 Barcelona, Spain

## HIGHLIGHTS

- SMPS data from a street canyon and downwind park locations.
- Modal analysis of size distributions at both sites.
- Particle size reduction of 22 nm mode to 6.2 nm average.
- Average shrinkage rate of 0.13 nm s<sup>−1</sup>.
- Consistent with semi-volatile composition of traffic nanoparticle emissions.

## ARTICLE INFO

### Article history:

Received 14 August 2015  
Received in revised form 22 October 2015  
Accepted 27 October 2015  
Available online 2 November 2015

### Keywords:

Nanoparticles  
Ultrafine particles  
Evaporation  
Particle size  
Semi-volatile

## ABSTRACT

Earlier work has demonstrated the potential for volatilisation of nanoparticles emitted by road traffic as these are advected downwind from the source of emissions, but there have been few studies and the processes have yet to be elucidated in detail. Using a dataset collected at paired sampling sites located respectively in a street canyon and in a nearby park, an in depth analysis of particle number size distributions has been conducted in order to better understand the size reduction of the semi-volatile nanoparticles. By sorting the size distributions according to wind direction and fitting log normal modes, it can be seen that the mode peaking at around 22 nm at the street canyon site is on average shrinking to 6.2 nm diameter at the park site which indicates a mean shrinkage rate for these particles of 0.13 nm s<sup>−1</sup> with temperatures within the range 12–18 °C. The diurnal variation of the shrunken mode in the park reflects the diurnal pattern of particle concentrations at the street canyon site taken as the main source area. An analysis of peak diameter for the smallest mode at the downwind park site shows an inverse relationship to wind speed suggesting that dilution rather than travel time is the main determinant of the particle shrinkage rate. An evaluation of previously collected C<sub>10</sub> to C<sub>35</sub> n-alkane data from a different urban location shows a good fit to Pankow partitioning theory reflecting the semi-volatility of compounds believed to be representative of the composition of diesel exhaust nanoparticles, hence confirming the feasibility of an evaporative mechanism for particle shrinkage.

© 2015 The Authors. Published by Elsevier Ltd.

This is an open access article under the CC BY license (<http://creativecommons.org/licenses/by/4.0/>).

## 1. Introduction

Road traffic is an appreciable source of particulate matter in the urban atmosphere, contributing both to particle mass across a

wide spectrum of particle sizes, and to particle number (Pant and Harrison, 2013; Charron and Harrison, 2003). In the latter context, studies at roadside show a huge elevation in particle number concentrations which declines rapidly with distance from the highway (e.g. Zhu et al., 2002a,b; Zhang et al., 2005). If the decline in particle number closely parallels that of conservative tracers such as carbon monoxide and black carbon, as was reported by Zhu et al. (2002a), it is likely that dilution processes are the primary determinant of concentrations. Some studies have, however, shown

\* Corresponding author. Also at: Department of Environmental Sciences/Center of Excellence in Environmental Studies, King Abdulaziz University, PO Box 80203, Jeddah 21589, Saudi Arabia.

E-mail address: [r.m.harrison@bham.ac.uk](mailto:r.m.harrison@bham.ac.uk) (R.M. Harrison).

a steeper gradient in particle number moving away from the highway than for other traffic-generated pollutants (Zhu et al., 2002b; Fushimi et al., 2008) and in this situation processes additional to dilution must be at play.

Measurements of particle size distributions as a function of distance from a highway source can be informative as to those processes which are involved. Such measurements typically show a faster decline in the nucleation mode particles (<ca 20 nm) than the accumulation mode (>ca 50 nm) (Fushimi et al., 2008; Sturm et al., 2003), but care is needed in interpreting this observation. As pointed out by Shi et al. (1999), the mixing of nucleation particle-rich air with background air containing mainly accumulation mode particles as air is advected from the highway will in itself lead to a reduction in the relative abundance of nucleation mode particles with distance from the highway. However, such processes can be considered in the data analysis by appropriate model design and/or measurements in the air upwind of the highway which provides the dilution air for the vehicle emissions.

Zhu et al. (2002b) observed a rapid drop in 6–25 nm particles with distance from a freeway, inferring evidence of coagulation processes affecting the smallest particles. A contribution from evaporation was not considered. Zhang et al. (2005) reported a large relative loss of sub-20 nm particles with distance from a freeway which they attributed to condensation/evaporation processes. They also reported a major influence of season upon particles in the 10–20 nm mode, with a substantial reduction seen in the warmer conditions of summer. This effect could influence either the initial formation of nucleation mode particles during the dilution of hot exhaust gases (Shi and Harrison, 1999; Charon and Harrison, 2003; Zhang et al., 2004) or be due to evaporation subsequent to emission. Fushimi et al. (2008) observed a sharp peak in winter with a modal diameter of ca 20 nm at roadside, which was not observed at a background site 200 m downwind. They interpreted their observations as being due to partial evaporation of semi-volatile organic compounds up to C<sub>35</sub> n-alkane in the atmosphere. In a subsequent study, Fujitani et al. (2012a) showed that in a summer study (31.2 °C), the <30 nm mode observed at roadside in winter was not observed, and that rapid loss of the <30 nm mode occurred in winter. In a simple calculation, they estimated that the complete evaporation of C<sub>10</sub>–C<sub>38</sub> n-alkanes would occur at the summer temperature. Given that laboratory studies have shown that the nucleation mode particles in diesel exhaust are mostly composed of alkanes and alkyl-substituted cycloalkanes from unburned fuels or engine oils (Tobias et al., 2001; Fushimi et al., 2011), such evaporative losses appear likely to explain many of the atmospheric observations.

Dall'Osto et al. (2011), reporting results from the REPAREE study (Harrison et al., 2012), analysed observations of particle size distributions from London (UK), reporting a reduction in the size of nucleation mode particles, both during advection from a major highway, and when dispersing vertically to a tower-based measurement site. The results were interpreted as showing evaporative loss of semi-volatile constituents causing a reduction in the diameter of traffic-generated nanoparticles during travel times of around 5 min. In this paper, we report a further analysis of results from the REPAREE experiments so as to better quantify the rate of size reduction of nucleation mode particles.

## 2. Methods

Previous work (Dall'Osto et al., 2011) recorded particle size spectra at three sites (roadside, urban park and tower) in London, and reported a large shift in particle size distributions with major concentration losses at the smallest sizes, as particles are advected

away from traffic sources. These authors examined simultaneously recorded particle size spectra at sizes greater than 14.9 nm from sites at Marylebone Road, Regent's Park and the BT Tower, and particle size spectra down to 3–5 nm which were not obtained simultaneously. It was concluded that semi-volatile traffic generated particles were reducing in size as they were advected from the roadside (Marylebone Road) to the parkland (Regent's Park), a distance of around 665 m. The data reported and analysed by Dall'Osto et al. (2011) included both simultaneously collected and non-simultaneously collected data from three sites, Marylebone Road, Regent's Park and BT Tower. In this paper, we use only the data from Marylebone Road and Regent's Park. Marylebone Road is a street canyon with a 6-lane highway carrying over 70,000 vehicles per day. The data were collected with a nano-SMPS system comprising a TSI model 3080N nanoclassifier and a model 3025 ultrafine condensation particle counter (CPC), covering the range 5–184 nm. The Regent's Park site is located in a central area of the park well away from significant motor traffic. Data were collected with a Differential Mobility Particle Sizer (DMPS) consisting of two "Vienna" style DMAs, an ultrafine DMA for particles of 3.4–34 nm and a standard DMA for particles of 30–830 nm. The former was connected to a TSI model 3025 ultrafine CPC and the latter to a TSI model 3010 CPC. Dall'Osto et al. (2011) explain how instrument inter-comparisons were conducted, and different datasets combined for analysis.

In the present work, the size spectra of smaller particles obtained at Marylebone Road and Regent's Park are examined in relation to the wind direction (measured at Heathrow). These data were obtained in the month of October 2003 and 2006 respectively at the two sites. The air sampling took place at a time when the fuel sulphur level was limited to 50 ppm and preceded the introduction of "zero sulphur" (<10 ppm S) diesel fuel which was mandatory for sale for use in diesel powered highway vehicles in the UK from 4 November 2007. The introduction of "zero sulphur" fuel resulted in a substantial reduction in the number concentration of ultrafine particulate matter (Jones et al., 2012) which may influence any comparison of particle size spectra obtained before and after this date. The locations of the sampling sites appear in Fig. 1.

### 2.1. Data treatment

The periods of measurement and equipment used at the Marylebone Road and Regent's Park sites are provided in detail by Dall'Osto et al. (2011). Hourly mean size spectra data were available for the Marylebone Road site. The data from the Regent's Park site was in 10-min means and this was used to calculate hourly mean values.

Hourly temperature and rainfall data were obtained from the central London meteorological station at St James's Park. Hourly wind speed and direction data are not available from this site, so were obtained from the meteorological station at Heathrow Airport to the west of London. This is 22.5 km from the sampling sites, but wind directions are usually fairly consistent over distances of up to 40 km (Manning et al., 2000), except in low wind speed conditions (Arciszewska and McClatchey, 2001).

## 3. Results and discussion

### 3.1. Overall spectra

The hourly Heathrow wind direction data were used to sort the hourly particle size spectra into eight 45° sectors based on the main compass points, and the mean spectra were calculated for both sites. These mean spectra are shown for Marylebone Road and

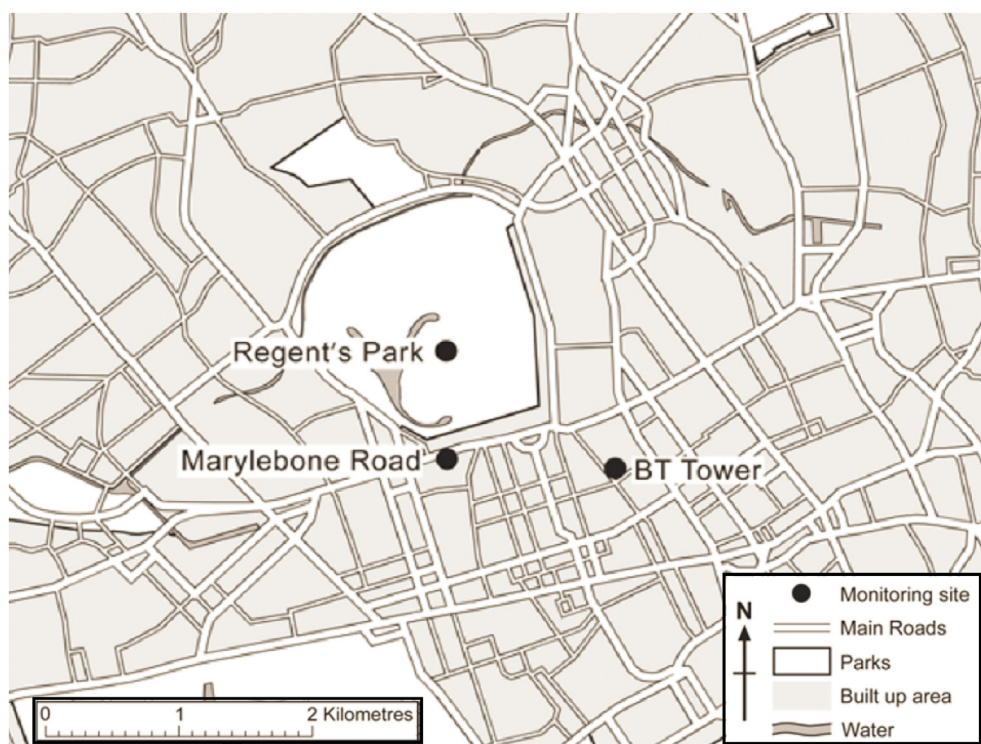


Fig. 1. Location of measurement sites.

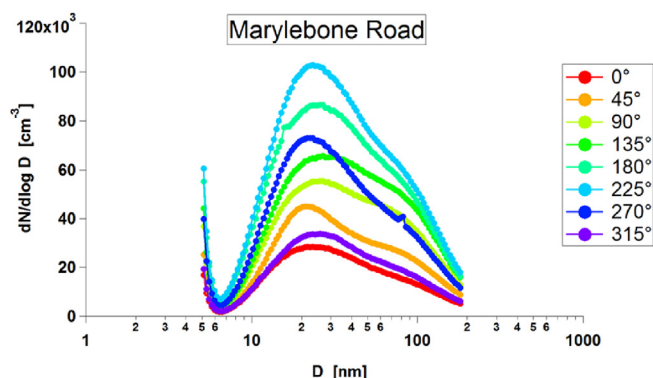


Fig. 2. Mean spectra obtained at different wind directions at Marylebone Road (October 2003).

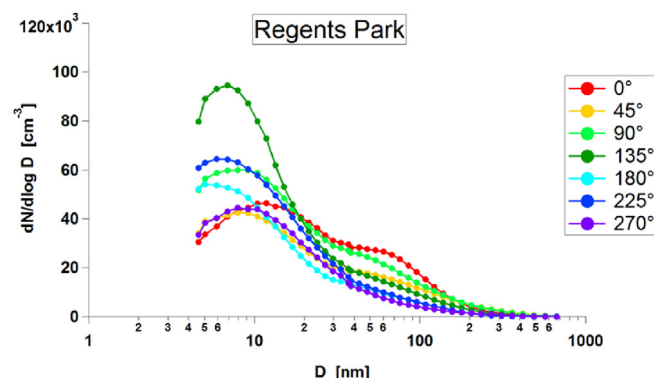


Fig. 3. Mean spectra obtained at different wind directions at Regent's Park (October 2006).

Regent's Park in Figs. 2 and 3 respectively. Due to the limited period of the observations no data was available for the 315° wind sector at Regent's Park.

At Marylebone Road (Fig. 2) the highest concentrations at 20–30 nm are associated with wind directions between 180° and 270° which are associated with the transport of material from the traffic passing to the north in the street canyon (due to the vortex circulation), or from the signalised road junction to the west (Jones and Harrison, 2006). The relatively enhanced concentrations around 70 nm at wind directions of 45°–135° may be associated with higher concentrations of background material in more stable easterly wind conditions. The upturn in the spectra at small particle diameters (<6 nm) is believed to be an instrumental artefact.

At Regent's Park (Fig. 3) the highest concentrations occur in south easterly (135°) winds at 7 nm. This high concentration may be associated with background material accumulating in stable south easterly winds. In southerly winds (180°) overall concentrations were lower, although the mean concentration in the smallest

measured size range was relatively higher. Concentrations at 225° fell between the two.

Modes were fitted to the mean spectra (excluding the sub 7 nm section of the Marylebone Road data) using the Igor Pro software package. The coefficients of the fitted modes are presented in Table 1 (a and b) for Marylebone Road and Regent's Park respectively. The fitted spectra for each wind sector at both sites are shown in Fig. S1.

### 3.2. Hourly spectra

Modes were fitted to the hourly data obtained at Regent's Park during south easterly (135°), southerly (180°) and south westerly winds (225°), and at Marylebone Road during southerly (180°) winds using the Igor Pro software package. These wind directions were selected as they would plausibly link the major line source of Marylebone Road with the downwind Regent's Park site. Initially, the number of modes fitted was arbitrarily determined by eye. In



**Table 1**

Characteristics of mean particle number size distributions for each wind sector; (a) Marylebone Road, (b) Regent's Park.

| Wind direction | First mode             |                   |                   | Second mode                |                        |                   |                   |
|----------------|------------------------|-------------------|-------------------|----------------------------|------------------------|-------------------|-------------------|
| Location (nm)  | Amplitude <sup>a</sup> | Area <sup>b</sup> | FWHM <sup>c</sup> | Location <sup>a</sup> (nm) | Amplitude <sup>a</sup> | Area <sup>b</sup> | FWHM <sup>c</sup> |
| (a)            |                        |                   |                   |                            |                        |                   |                   |
| 0°             | 20.7                   | 25,211            | 874,312           | 29.8                       | 68.2                   | 14,534            | 2,151,980         |
| 45°            | 20.3                   | 39,857            | 1,130,000         | 25.0                       | 69.3                   | 26,044            | 3,620,000         |
| 90°            | 22.5                   | 51,747            | 2,132,430         | 35.0                       | 79.1                   | 34,985            | 4,748,530         |
| 135°           | 24.2                   | 63,291            | 3,026,510         | 40.1                       | 85.1                   | 39,314            | 5,359,370         |
| 180°           | 22.5                   | 83,737            | 3,679,850         | 37.0                       | 80.6                   | 44,345            | 5,960,260         |
| 225°           | 22.5                   | 99,658            | 4,103,940         | 35.0                       | 80.8                   | 49,666            | 6,609,210         |
| 270°           | 20.7                   | 66,974            | 2,196,600         | 28.4                       | 69.5                   | 36,756            | 4,952,040         |
| 315°           | 23.8                   | 32,916            | 1,436,150         | 37.1                       | 85.5                   | 14,542            | 1,986,790         |
| (b)            |                        |                   |                   |                            |                        |                   |                   |
| 0°             | 11.1                   | 46,198            | 1,975,870         | 31.0                       | 72.1                   | 16,886            | 1,934,160         |
| 45°            | 7.6                    | 42,024            | 925,880           | 17.2                       | 57.5                   | 14,076            | 2,463,590         |
| 90°            | 7.4                    | 60,622            | 1,408,530         | 17.8                       | 54.6                   | 18,019            | 2,613,740         |
| 135°           | 6.6                    | 91,891            | 1,293,470         | 11.7                       | 35.7                   | 16,280            | 2,084,590         |
| 180°           | 5.9                    | 54,255            | 1,055,440         | 14.7                       | 54.6                   | 7994              | 934,407           |
| 225°           | 6.4                    | 64,509            | 1,738,660         | 19.1                       | 77.0                   | 4693              | 610,392           |
| 270°           | 8.6                    | 44,361            | 1,228,940         | 21.0                       | 63.7                   | 3606              | 672,498           |
| 315°           | no data                | no data           | no data           | no data                    | no data                | no data           | no data           |

<sup>a</sup> Amplitude is  $\text{dN}/\text{dlogD}$  ( $\text{cm}^{-3}$ ) at the mode of the distribution.<sup>b</sup> Area is that under the lognormal curve ( $\text{nm cm}^{-3}$ ).<sup>c</sup> FWHM is an expressions of the width of the lognormal curve (Full Width at Half Maximum Height).

order to be more systematic and ensure that a mode was fitted to the high concentrations at small particle sizes, the process was started offering two modes between 5 nm and 100 nm, the background was set at zero, and modes with negative positions or amplitudes were rejected. Additional modes were only included if necessary to achieve a fit to the data - during one case out of 118 in the Regent's Park data, and 14 cases out of 126 in the Marylebone Road data. Starting the process with a small mode at 5 nm ensured that a mode was fitted to the curve at small particle diameters at the Regent's Park site. The coefficients of the fitted modes are presented in Table S1, with selected examples of spectra shown in Fig. 4. These examples are chosen for both sites at hours starting 07:00 and 15:00, wind directions between 170° and 190°, and wind speeds of 4.6–5.2  $\text{m s}^{-1}$ .

The modal diameters identified in the hourly data for both sites in the 180° wind sector, and for the 135° and 225° wind sectors

at Regent's Park, were sorted into ten logarithmic bins per order of magnitude and the normalised probability density function was calculated, and is plotted against the lower band diameter in Fig. 5. While the modal distribution is similar for the three wind sectors at Regent's Park with most identified modes occurring around particle diameters of 7 nm and 70 nm, the plot for the Marylebone Road site (180° wind sector) shows two broad peaks (one bimodal) with zero occurrence below around 10 nm. This clearly shows a small reduction in size of the coarser mode at Marylebone Road, but a much larger reduction in the smaller (ca 30 nm) mode when the particles are sampled at Regent's Park.

### 3.3. Relationship of mode amplitude to time of day

The amplitudes and diameters of the two modes in the individual hourly spectra in the data from Regent's Park replotted against

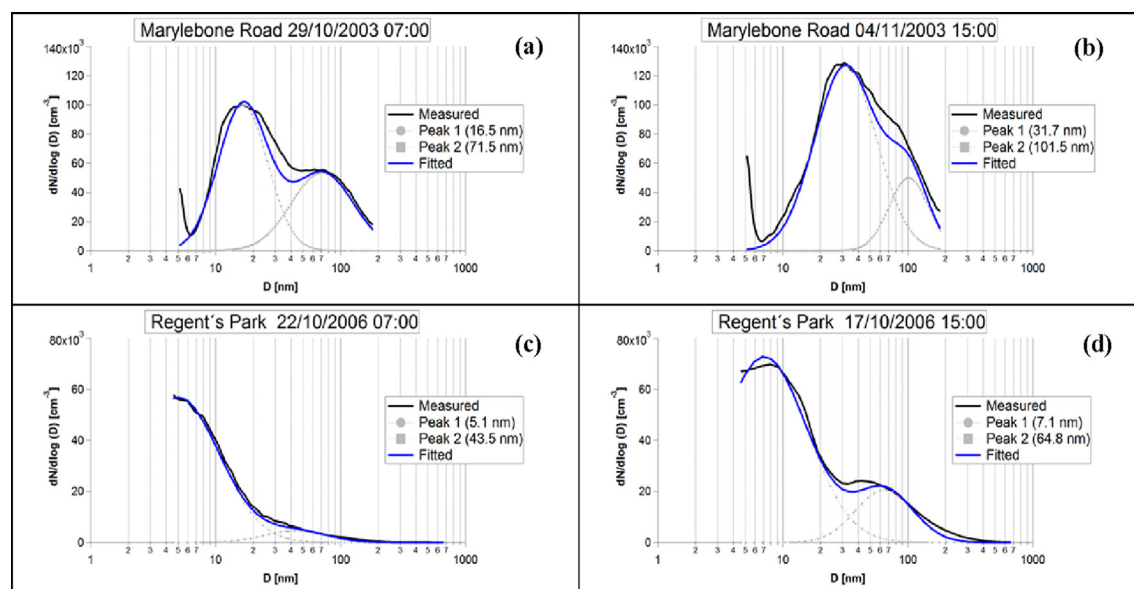


**Fig. 4.** Examples of hourly spectra at Marylebone Road and Regent's Park during southerly winds at wind speeds of 4.6–5.2  $\text{m s}^{-1}$  in morning and mid-afternoon: (a) Marylebone Road 07:00; (b) Marylebone Road 15:00; (c) Regent's Park 07:00; (d) Regent's Park 15:00.

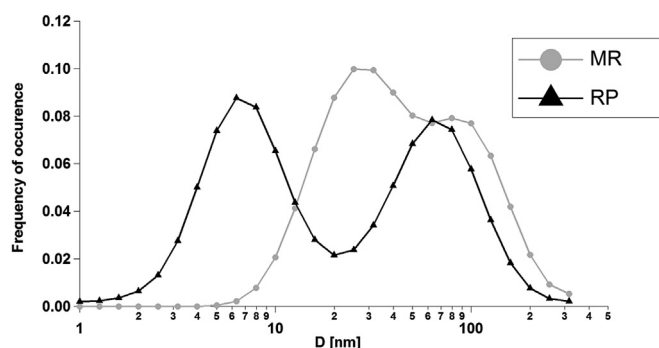


Fig. 5. Probability of identified modes at Marylebone Road (MR) and Regent's Park (RP).

time of day in Figure S2a–d. In the case of the lower mode amplitudes (Figure S2a) there is evidence of a diurnal profile typical of traffic generated pollutants with minimum concentrations overnight, a rapid rise around the morning commuting period, and gradually reducing concentrations over the working day. This is partially obscured by a number of low amplitude data points, which may be a result of modes being fitted to minor perturbations in the spectra, and more scattered data in the 135° wind direction. This temporal pattern confirms local road traffic as the probable predominant source of the smaller particle mode at Regent's Park and rules out regional nucleation processes as an important source, as this mode is seen to occur in hours of darkness. A correlation with carbon monoxide was previously taken as indicative of a road traffic source (Dall'Osto et al., 2011). Two events occurring between 12 and 15 h (Figure S2a) may reflect nucleation processes taking place in the Park.

In a similar manner, the amplitudes and diameters of the first and second modes at Marylebone Road are plotted against time of day in Figure S3a–b. A similar diurnal variation to that seen for the smaller modes at Regent's Park is apparent in the mode amplitudes of both modes at Marylebone Road (Figure S3a–b). Diurnal trends are not present in the mode diameters of either size range at Marylebone Road (Figure S3c–d).

### 3.4. Relationship of mode amplitude and diameter to meteorological conditions

The mode amplitudes and diameters of the individual hourly spectra in the first and second modes were plotted against wind speed, air temperature and relative humidity. Correlations were poor and there was no obvious relationship between the mode amplitude or diameter and any of the meteorological conditions considered, with the exception of the diameter of the first mode at Regent's Park, where there is a general reduction of diameter with wind speed when data from all three wind directions is considered (Fig. 6). The most obvious effect of an increased wind speed is to decrease travel time between the source and receptor, hence giving less time for evaporation to take place. Thus the result is counter-intuitive at first sight. However, the other effect of increased wind speed will be to increase turbulence and dilution, which may have the effect of more rapid dilution of the vapour component, hence increasing the concentration gradient between the vapour pressure at the particle surface and in the ambient air, hence enhancing the rate of evaporation. This explanation is supported by analysis of the relationship between  $\text{NO}_x$  concentration measured at the Regent's Park site and wind speed. These variables were negatively correlated for all wind directions, confirming the likelihood of dilution of hydrocarbon vapours. No such effect of wind speed upon the Marylebone Road

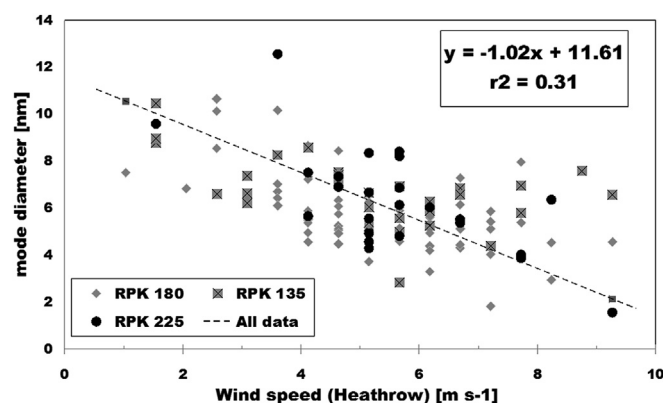


Fig. 6. Diameters of first mode at Regent's Park as a function of wind speed.

data was seen, but the site is in a street canyon, which will not respond in the same way to changes in wind speed external to the canyon.

No influence of relative humidity or air temperature on the small mode diameter at Regent's Park was evident, but the range of air temperatures was small (12–18 °C) in comparison to earlier studies using seasonal contrasts.

The Regent's Park measurement site is approximately 665 m north of the air quality site on Marylebone Road. Over the full range of plausible wind directions, the distance ranges from 600 to 780 m. The wind speed measurements used were obtained from measurements made at Heathrow Airport to the west of London – at a site not affected by nearby buildings – at a nominal height of 10 m above ground level. Wind speeds in central London are likely to be less, although much of the land between the sites at Marylebone Road and Regent's Park is within the park, and the wind speed at locations between these sites is not likely to be greatly affected by nearby buildings. Wind speed also varies rapidly with height close to the ground and during advection between the two sites the sampled volume of air may have been mixed across a range of heights, particularly at the relatively high mean wind speed (measured at Heathrow) of  $5.3 \text{ m s}^{-1}$  that was observed during the period of southerly winds during sampling at the Regent's Park site.

In the absence of any more reliable measurement of wind speed from that obtained at Heathrow, the reduction of size of the dominant mode from a mean of 22.0 nm at Marylebone Road to 6.2 nm at Regent's Park, indicates a mean shrinkage rate for these particles of  $0.13 \text{ nm s}^{-1}$ . There is clearly a substantial range around this value, dependent upon wind direction, speed, dilution and air temperature. Fig. 6 shows no consistent dependence upon wind direction, and the dataset is too small to allow a multivariate analysis of the influential factors.

### 3.5. Plausibility of evaporative processes

The chemical composition of diesel exhaust nanoparticles has not been defined in detail. Tobias et al. (2001) used a differential mobility analyser to size-select nanoparticles of 25–60 nm from diesel exhaust for analysis by a thermal desorption particle beam mass spectrometer. They reported that alkanes and alkyl-substituted cycloalkanes from unburned fuel and lubricating oil appeared to be the major constituents. Fushimi et al. (2008, 2011) used GC-MS methods to analyse diesel exhaust and atmospheric nanoparticles, reporting complex mixtures with clear peaks due to n-alkanes predominantly within the range  $\text{C}_{10}$  to  $\text{C}_{35}$ . Much of the material in the chromatograms was not resolved by the GC separation, but came within the volatility range of the  $\text{C}_{20}$  to

C<sub>25</sub> n-alkanes. Both Lipsky and Robinson (2006) and Fujitani et al. (2012b) have shown that hydrocarbons are lost from diesel exhaust particles during dilution with clean air in the laboratory. Their work is concerned primarily with changes in the mass of particle emissions in the accumulation mode, i.e. in particles which comprise largely elemental carbon and are much larger than those studied in our work. Their results do not allow inference of the rate of mass loss and hence of size distribution changes in particles in the sub-50 nm range. Fujitani et al. (2012b) highlight the semi-volatility of n-alkanes in the range of C<sub>16</sub>–C<sub>24</sub>. The composition of the nanoparticles measured in our study is unknown, but our data below establish the semi-volatile nature of n-alkanes up to C<sub>34</sub>.

We have analysed a dataset for n-alkanes in urban air measured in 1999 and 2000 by Harrad et al. (2003). The air samples were collected at a roadside site in Birmingham, UK (Bristol Road) and an urban background site (campus) and were analysed for separate particle-associated and vapour fractions. Following the widely adopted method for analysis of data for semi-volatile compounds (Pankow and Bidleman, 1992; Pankow, 1994), the partition coefficient, K<sub>p</sub> was calculated from:

$$K_p = (C_p/TSP)/C_g \quad (1)$$

In which C<sub>p</sub> is the concentration in the particulate phase, C<sub>g</sub> the concentration of vapour and TSP is the total suspended particle concentration. Log K<sub>p</sub> was regressed against vapour pressure (VP<sub>T</sub>) for the relevant temperature derived from EPI Suite v1.43 according to the following equation:

$$\text{Log } K_p = m \log(\text{VP}_T) + b \quad (2)$$

This was conducted in two ways. Firstly, as is conventional, log K<sub>p</sub> was regressed upon log (VP<sub>T</sub>) pooling data for all hydrocarbons (C<sub>16</sub> to C<sub>34</sub>) on a given day. Data from both sites were combined and the results appear in Table S2. Over a substantial range of compounds and temperatures (3.0–18.3 °C), a good fit to the data (r<sup>2</sup> = 0.55–0.91) was found. A more demanding analysis (due to the smaller range of vapour pressures) was to take compounds individually and pool the data from all days, with results appearing in Table S3. In this case, the gradients show a much wider range, and many of the r<sup>2</sup> values are very low, and not significant (p < 0.05 for r<sup>2</sup> > 0.16). However, for six more abundant compounds with concentrations measured with greater precision in both particle and vapour phases (C<sub>19</sub> to C<sub>24</sub>), r<sup>2</sup> values range from 0.32 to 0.57, showing a reasonable fit.

From this analysis, we conclude that n-alkanes present in diesel exhaust particles and representative of the volatility range of the many compounds in both diesel exhaust and ambient airborne particles, are actively partitioning between particle and vapour as temperature changes. Dilution with cleaner air also influences the partitioning as demonstrated in laboratory studies by Lipsky and Robinson (2006) and Fujitani et al. (2012b). Semi-volatile compounds would hence tend to pass from the condensed phase to vapour as air is advected from the highly polluted Marylebone Road to the much cleaner environment of Regent's Park, with the exception of those compounds having a strong, probably biogenic, source within the park.

#### 4. Conclusions

The amplitudes of both modes at Marylebone Road, and the smaller mode at Regent's Park, show an increase in concentration at around 08:00 h (Figs. S2 and S3) and are probably both influenced by the increase in the concentration of traffic emissions which occurs around this time. It is likely that these modes are due to traffic emissions. The reduction in size of the dominant smaller mode between the two sites indicates a shrinkage rate of

0.13 nm s<sup>−1</sup>. This is expected to show some temperature dependence, but the range of temperatures in our study was quite small (12–18 °C) and this influence is not seen.

No systematic relationship was found between mode amplitude or diameter and air temperature or relative humidity at either site. Any relationship between mode diameter and inverse wind speed (related to time of travel) is heavily influenced by a small number of occasions of particularly low wind speeds. The most rapid evaporation appears to occur at higher wind speeds, associated with shorter travel times, but cleaner air. Analysis of a separate dataset for Birmingham demonstrates the active partitioning of C<sub>16</sub> to C<sub>34</sub> n-alkanes (associated with diesel exhaust) between the condensed phase and vapour, hence supporting the concept of evaporative shrinkage of nanoparticles.

#### 5. Acknowledgements

Primary collection of nanoparticle data took place during the REPARTEE project which was funded by the Natural Environment Research Council through the National Centre for Atmospheric Science (R8/H12/83/011) and the BOC Foundation. The collection of hydrocarbon data was supported by the Natural Environment Research Council (Grant Ref GR3/11371). Data analyses were carried out with support from the European Research Council as part of the FASTER project (Ref Proposal No. 320821). The authors would like to acknowledge the support of the National Centre for Atmospheric Science (NCAS) and the Atmospheric Measurement Facility (AMF) for the use of DMPS data.

#### Appendix A. Supplementary data

Supplementary data related to this article can be found at <http://dx.doi.org/10.1016/j.atmosenv.2015.10.077>.

#### References

- Arciszewska, C., McClatchey, J., 2001. The importance of meteorological data for modelling air pollution using ADMS-Urban. *Meteorol. Appl.* 8, 343–350.
- Charron, A., Harrison, R.M., 2003. Primary particle formation from vehicle emissions during exhaust dilution in the roadside atmosphere. *Atmos. Environ.* 37, 4109–4119.
- Dall'Osto, M., Thorpe, A., Beddows, D.C.S., Harrison, R.M., Barlow, J.F., Williams, P.I., Coe, H., 2011. Remarkable dynamics of nanoparticles in the urban atmosphere. *Atmos. Chem. Phys.* 11, 6623–6637.
- Fushimi, A., Hasegawa, S., Takahashi, K., Fujitani, Y., Tanabe, K., Kobayashi, S., 2008. Atmospheric fate of nuclei-mode particles estimated from the number concentrations and chemical composition of particles measured at roadside and background sites. *Atmos. Environ.* 42, 949–959.
- Fushimi, A., Saitoh, K., Fujitani, Y., Hasegawa, S., Takahashi, K., Tanabe, K., Kobayashi, S., 2011. Organic-rich nanoparticles (diameter: 10–30 nm) in diesel exhaust: fuel and oil contribution based on chemical composition. *Atmos. Environ.* 45, 6326–6336.
- Fujitani, Y., Kumar, P., Tamura, K., Fushimi, A., Hasegawa, S., Takahashi, K., Tanabe, K., Kobayashi, S., Hirano, S., 2012. Seasonal differences of the atmospheric particle size distribution in a metropolitan area in Japan. *Sci. Total Environ.* 437, 339–347.
- Fujitani, Y., Saitoh, K., Fushimi, A., Takahashi, K., Hasegawa, S., Tanabe, K., Kobayashi, S., Furuyama, A., Hirano, S., Takami, A., 2012. Effect of isothermal dilution on emission factors of organic carbon and n-alkanes in the particle and gas phases of diesel exhaust. *Atmos. Environ.* 59, 389–397.
- Harrad, S., Hassoun, S., Callen Romero, M.S., Harrison, R.M., 2003. Characterisation and source attribution of the semi-volatile organic content of atmospheric particles and associate vapour phase in Birmingham, UK. *Atmos. Environ.* 37, 4985–4991.
- Harrison, R.M., Dall'Osto, M., Beddows, D.C.S., Thorpe, A.J., Bloss, W.J., Allan, J.D., Coe, H., Dorsey, J.R., Gallagher, M., Martin, C., Whitehead, J., Williams, P.I., Jones, R.L., Langridge, J.M., Benton, A.K., Ball, S.M., Langford, B., Hewitt, C.N., Davison, B., Martin, D., Petersson, K., Henshaw, S.J., White, I.R., Shallcross, D.E., Barlow, J.F., Dunbar, T., Davies, F., Nemitz, E., Phillips, G.J., Helfter, C., Di Marco, C.F., Smith, S., 2012. Atmospheric chemistry and physics in the atmosphere of a developed megacity (London): an overview of the REPARTEE experiment and its conclusions. *Atmos. Phys. Chem.* 12, 3065–3114.
- Jones, A.M., Harrison, R.M., 2006. Estimation of the emission factors of particle number and mass fractions from traffic at a site where mean vehicle speeds vary over short distances. *Atmos. Environ.* 40, 7125–7137.

- Jones, A.M., Harrison, R.M., Barratt, B., Fuller, G., 2012. A large reduction in airborne particle number concentrations at the time of the introduction of “sulphur free” diesel and the London Low Emission Zone. *Atmos. Environ.* 50, 129–138.
- Lipsky, E.M., Robinson, A.L., 2006. Effects of dilution on fine particle mass and partitioning of semivolatile organics in diesel exhaust and wood smoke. *Environ. Sci. Technol.* 40, 155–162.
- Manning, A.J., Nicholson, K.J., Middleton, D.R., Rafferty, S.C., 2000. Field study of wind and traffic to test a street canyon pollution model. *Environ. Monit. Assess.* 60, 283–313.
- Pankow, J.F., Bidleman, T.F., 1992. Interdependence of the slopes and intercepts from log-log correlations of measured gas-particle partitioning and vapour pressure – I. Theory and analysis of available data. *Atmos. Environ.* 26A, 1071–1080.
- Pankow, J.F., 1994. An absorption model of gas/particle partitioning of organic compounds in the atmosphere. *Atmos. Environ.* 28, 185–188.
- Pant, P., Harrison, R.M., 2013. Estimation of the contribution of road traffic emissions to particulate matter concentrations from field measurements: a review. *Atmos. Environ.* 77, 89–97.
- Shi, J.P., Khan, A.A., Harrison, R.M., 1999. Measurements of ultrafine particle concentration and size distribution in the urban atmosphere. *Sci. Total Environ.* 235, 51–64.
- Shi, J.P., Harrison, R.M., 1999. Investigation of ultrafine particle formation during diesel exhaust dilution. *Environ. Sci. Technol.* 33, 3730–3736.
- Sturm, P.J., Baltensperger, U., Bacher, M., Lechner, B., Hausberger, S., Heiden, B., Ihof, D., Weingartner, E., Prevot, A.S.H., Kurtenbach, R., Wiesen, P., 2003. Roadside measurements of particulate matter size distribution. *Atmos. Environ.* 37, 5273–5281.
- Tobias, H.J., Beving, D.E., Ziemann, P.J., 2001. Chemical analysis of diesel engine nanoparticles using a nano-DMA/thermal desorption particle beam mass spectrometer. *Environ. Sci. Technol.* 35, 2233–2243.
- Zhang, K.M., Wexler, A.S., Zhu, Y.F., Hinds, W.C., Sioutas, C., 2004. Evolution of particle number distributions near roadways Part II: the road-to-ambient process. *Atmos. Environ.* 38, 6655–6665.
- Zhang, K.M., Wexler, A.S., Niemeier, D.A., Zhu, Y.F., Hinds, W.C., Sioutas, C., 2005. Evolution of particle number distribution near roadways. Part II: traffic analysis and on-road size resolved particulate emission factors. *Atmos. Environ.* 39, 4155–4166.
- Zhu, Y., Hinds, W.C., Kim, S., Shen, S., Sioutas, C., 2002. Study of ultrafine particles near a major highway with heavy-duty diesel traffic. *Atmos. Environ.* 36, 4323–4335.
- Zhu, Y., Hinds, W.C., Kim, S., Sioutas, C., 2002. Concentration and size distribution of ultrafine particles near a major highway. *J. Air Waste Manag. Assoc.* 52, 1032–1042.